Title

Basic fibroblast growth factor uniquely stimulates quiescent vascular smooth muscle cells and induces proliferation and dedifferentiation

Kiyomi Tsuji-Tamura* **and Masato Tamura**

Oral Biochemistry and Molecular Biology, Department of Oral Health Science, Faculty of Dental Medicine and Graduate School of Dental Medicine, Hokkaido University, Kita 13, Nishi 7, Kita-ku, Sapporo 060-8586, Japan

*Author for correspondence: Kiyomi Tsuji-Tamura

Mailing address: Oral Biochemistry and Molecular Biology, Department of Oral Health Science, Faculty of Dental Medicine and Graduate School of Dental Medicine, Hokkaido University, Kita 13, Nishi 7, Kita-ku, Sapporo 060-8586, Japan

E-mail: ktamuratsuji@den.hokudai.ac.jp

Tel: +81-11-706-4243

Keywords

Cell quiescence; vascular smooth muscle cells; vascular endothelial cells; bFGF; TGFβ1; TAGLN

Abbreviations

SMCs: Vascular smooth muscle cells

ECs: Vascular endothelial cells

BMP4: Bone morphogenetic protein 4

CXCL12: Chemokine (C-X-C motif) ligand 12

EPO: Erythropoietin

FGFa: Fibroblast growth factor acidic

bFGF: Basic fibroblast growth factor

IGF-II: Insulin-like growth factor-II

IL-3: Interleukin-3

PDGF-BB: Platelet derived growth factor-BB

SCF: Stem cell factor

SHH: Sonic hedgehog

TGFβ1: Transforming growth factor beta 1

VEGF: Vascular endothelial growth factor 165

WNT-3A: Wingless-type MMTV integration site family, member-3A

TAGLN: Transgelin

Fgfr1: FGF receptor 1

B2m: β-2 microglobulin

Gapdh: glyceraldehyde-3-phosphate dehydrogenase

Srf: serum response factor

Klf4: Kruppel-like factor 4

Abstract

Blood vessels normally remain stable over the long-term. However, in atherosclerosis, vascular cells leave quiescent state and enter activated state. Here, we investigated the factors that trigger breakage of quiescent state by screening growth factors and cytokines using a vascular smooth muscle cell (SMC) line and an endothelial cell (EC) line. Despite known functions of the tested factors, only basic fibroblast growth factor (bFGF) was identified as a potent trigger of quiescence breakage in SMCs, but not ECs. bFGF disrupted tight SMC-monolayers, and caused morphological changes, proliferation and dedifferentiation. Human primary SMCs, but not ECs, also showed similar results. Aberrant SMC-proliferation is a critical event in atherosclerosis. We thus provide further insights into the role of bFGF in vascular pathobiology.

Introduction

Vascular blood vessels are lined with a single layer of ECs and surrounded by layers of SMCs (for a review, see [1]). In healthy adult tissues, SMCs and ECs are stable and have a long lifespan. The half-life of SMCs isolated from the mouse aorta ranged from 270 to 400 days [2]. The turnover time of ECs obtained from mouse normal tissues ranged from 47 to 23,000 days [3]. Nevertheless, following chronic exposure of vessels to cardiovascular stress (e.g., dyslipidemia, hyperglycemia, or hypertension), vascular cells leave the quiescent state and become active (for reviews see [4] [5] [6] [7]). Aberrant EC activity occurs, and the release of various factors leads to further cell activation. The proliferation of dedifferentiated SMCs and lipid deposits thicken the intima of arteries. The vessels become narrow and hard, and eventually dysfunctional. This condition is termed atherosclerosis, and can lead to heart attack, heart failure, or stroke. Therefore, the vascular cell transition plays an important role in the initiation of atherosclerosis.

Cells have unique properties in the quiescent or proliferative state. Confluence and/or serum-deprived culture induced growth arrest and cellular quiescence, and caused distinct changes in gene expression in the mouse fetal fibroblast C3H10T1/2 cell line [8]. Expression of growth factor receptors was low in rabbit aortic SMCs, which formed a confluent layer within a short period [9]. bFGF-induced migration activities increased in rat aortic SMCs cultured after confluence, compared to those of SMCs maintained in the logarithmic phase [10]. Rabbit thoracic aortic SMCs in confluent cultures treated with bFGF showed increased expression of the VEGF gene in a time–dependent manner [11]. Sub-confluent and confluent human umbilical vein endothelial cells (HUVECs) showed cell density–dependent expression of numerous genes [12]. Therefore, it is necessary to investigate the effects of factors in the quiescent phase in addition to the growth phase.

Despite the availability of many studies on vascular cells (for a review, see [1]), the precise molecular cues involved in the switching from an inactive quiescent state to an active proliferative state are still unknown. *In vitro* studies under identical conditions are suitable for the validation of factors in the two

types of vascular cells. However, in most protocols, cells are maintained under varied culture conditions, including different specific media, serum and growth factor supplementation, and extracellular matrix. Serum deprivation is useful in the induction of the quiescent state and for the examination of molecular signaling; however, this condition is not tolerated by many *in vitro* models. Therefore, the aim of this study is to identify a trigger factor that breaks the quiescence of vascular cells by comparing the SMC and EC lines, which are maintained under the same conditions and can adapt to serum deprivation.

Materials and Methods

Cell cultures

The mouse aorta SMC line MOVAS (#CRL-2797, American Type Culture Collection, Manassas, VA, USA), mouse EC line UV♀2 (UV2) (#RCB1994, RIKEN BioResource Research Center, Tsukuba, Japan) and mouse melanoma cell line B16 (#RCB1283, RIKEN BioResource Research Center) were maintained in Dulbecco's Modified Eagle's Medium (Invitrogen, Grand Island, NY, USA) containing 10% fetal bovine serum (FBS) (growth medium).

Human aortic smooth muscle cells (AoSMCs) (#CC-2571, Lonza, MD USA) were cultured in Smooth Muscle Cell Growth Medium 2 (#C-22062, Takara Bio Inc., Shiga, Japan). HUVECs (Human umbilical vein endothelial cells) (#C2519A; Lonza) were cultured in Endothelial Cell Growth Medium Kit (#C-22110; Takara Bio Inc.) on gelatin-coated plates. AoSMCs and HUVECs from passage 3 to 7 were used for studies.

Antibodies and factors

The mouse monoclonal antibody against β–catenin (#SAB4200720, Sigma–Aldrich, St. Louis, MO, USA, 1:1000), the rabbit polyclonal against transgelin (TAGLN) (#ab14106, Abcam, Cambridge, UK,

1:1000) and Phalloidin-iFluor 488 Reagent (#ab176753, Abcam, 1:1000) were used. Although the anti-TAGLN antibody may recognize other TAGLN isoforms [13], it is referred to as TAGLN antibody in this article as shown in the datasheet. Alexa Fluor 546- (#A-11035) and Alexa Fluor 647- (#A32728) conjugated secondary antibodies (Invitrogen, Carlsbad, CA, USA) were used. Recombinant mouse (rm) chemokine (C-X-C motif) ligand 12 (CXCL12, also shown as SDF-1a) (BioLegend, San Diego, CA, USA) and recombinant human (rh) platelet derived growth factor (PDGF)-BB (Austral Biologicals, San Ramon, CA, USA) were used. Rh erythropoietin (EPO) was obtained from Kyowa Hakko Kirin (Tokyo, Japan). Rh FGF acidic (FGFa also known as FGF1), rm bFGF (also known as FGF2), rm sonic hedgehog (SHH), and rm wingless-type MMTV integration site family, member-3A (WNT-3A) were obtained from Novus Biologicals (Littleton, CO, USA). Recombinant human/mouse/rat ACTIVIN-A, rm bone morphogenetic protein 4 (BMP4), rm insulin-like growth factor-II (IGF-II) and rh transforming growth factor β1 (TGFβ1) were obtained from R&D Systems (Minneapolis, MN, USA). Rm interleukin-3 (IL-3), rm stem cell factor (SCF), and rm vascular endothelial growth factor 165 (VEGF) were purchased from PeproTech (Rocky Hill, NJ, USA).

Screening for quiescence breakage

Cells were cultured in each growth medium until confluence; the medium was replaced with Human Endothelial-Serum Free Medium (Gibco, Grand Island, NY, USA) (serum-free medium) with a tested factor (refer to text field). For human primary cells, Human Endothelial-Serum Free Medium (Gibco) with 0.1% FBS (low serum medium) was used to induce quiescence. After three days of culture, images of the monolayer of MOVAS and UV2 cells were captured using the live-cell imaging microscopy system IncuCyto Zoom (Essen BioScience, Ann Arbor, MI, USA). For human primary cells, microscope ECLIPSE TS100 (Nikon, Tokyo, Japan) was used to capture images. For a clear observation of the cell morphology, adjustments of brightness and contrast were uniformly applied to the original image using the ImageJ software version 1.440 (National Institutes of Health [NIH], Bethesda, MD, USA). The cell numbers were manually counted.

Fluorescent staining and analysis

Cells were fixed in 2% paraformaldehyde in phosphate-buffered saline (PBS) for 15 min at 37 °C. After washing in PBS, the fixed cells were incubated with a blocking buffer containing 0.1% Triton X-100 and 2% skim milk in PBS for 2 h at room temperature; this was followed by incubation with the aforementioned primary antibodies in a blocking buffer overnight at 4 °C. After washing in blocking buffer, the cells were incubated with fluorescent-labeled secondary antibodies for 2 h at room temperature. 4',6-diamidino-2-phenylindole (DAPI, Sigma–Aldrich) was used for the counterstaining of nuclei. Fluorescence images were captured using the FV1000D confocal laser scanning microscope and imaging software (Olympus, Tokyo, Japan). For a clear observation of the cell morphology, adjustments of brightness and contrast were uniformly applied to the original image. Imaging data were analyzed using the ImageJ software (NIH). Cell size and cell-free area were measured through manual tracing. Cell number was determined according to the number of DAPI-stained nuclei in each image. Co-localization area of TAGLN and actin was calculated based on the value of "the merged area of TAGLN and actin"/ "total actin area" in each image.

Luciferase reporter assay

The *Tagln* promoter [14] was amplified from the mouse genome by polymerase chain reaction (PCR) using the following primers: forward 5'-GCTCGCTAGCCTCGA AGTCAAGACTAGTTCCCACC-3' and reverse 5'-AGGCCAGATCTTGATGGGGCGCCGGCTGGGTGAGG-3' (the In-Fusion sites are underlined). The PCR product was inserted into the multi-cloning site of a pGL4.15 firefly luciferase reporter vector (Promega, Madison, WI, USA) using the In-Fusion HD Cloning Kit (Takara Bio Inc.). A pGL4.15 plasmid was co-transfected with pRL-SV40 (Promega) into MOVAS or UV2 cells using Xfect mESC Transfection Reagent (Clontech, Palo Alto, CA, USA) according to the instructions provided by the manufacturer. Following transfection, the cells were incubated in serum-free medium for two days and prepared using the Dual-Luciferase Reporter Assay System (Promega). Luciferase activity was measured using the GloMax-Multi Luminescence System (Promega).

Quantitative real-time PCR

Total RNA was extracted from the cells using the RNeasy Plus Mini kit (Qiagen, Venlo, Netherlands) and subjected to reverse transcription using the Omniscript Reverse Transcription kit (Qiagen). The relative quantification of gene expression was performed using QuantiTect SYBR Green PCR kits (Qiagen) or Thunderbird Probe qPCR Mix (TOYOBO, Osaka, Japan) in the StepOne real time PCR system (ABI, Foster City, CA, USA). The primer sequences for mouse FGF receptor 1 (*Fgfr1*) were: forward 5'-AGCAGTTGGTGGAAGACCTG-3', reverse 5'-GTACTGGTCCAGCGGTATGG-3'; and for mouse β-2 microglobulin (*B2m*): forward 5'-CTGACCGGCCTGTATGCTAT-3', reverse 5'-CCGTTCTTCAGCATTTGGAT-3'. The probe and primer sequences used for mouse *Tagln* were: probe 5'-AAGAGGGACTTCACAGACAGCCAACTGC-3', forward 5'-ATCCCAACTGGTTTATGAAGdAAAGC-3', reverse 5'-AAGGCCAATGACGTGCTTCC-3'; Kruppel-like factor 4 (*Klf4*): probe 5'-ACCAAGAGTTCTCATCTCAAGGCACACCTG-3', forward 5'-ACTTGTGACTATGCAGGCTGTG-3', reverse 5'-GGTTTCTCGCCTGTGTGAGTT-3'; mouse *B2m*: probe 5'-ACCGGCCTGTATGCTATCCAGAAAACCC-3', forward 5'-GGTCTTTCTGGTGCTTGTCTCA-3', reverse 5'-GTTCGGCTTCCCATTCTCCG-3'. Predesigned primer and probe sets (TaqMan Gene Expression Assays; ABI) were used for the detection of mouse serum response factor (*Srf*) or mouse glyceraldehyde-3-phosphate dehydrogenase (*Gapdh*) gene. The primer sequences for human *TAGLN* were: forward 5'-GCAAAGACATGGCAGCAGT-3', reverse 5'-GCTGGCTCTCTGTGAATTCC-3'; human *SRF*: forward 5'-ATCTGGGACAGTGCAGATCC-3', reverse 5'-CACCTGTAGCTCGGTGAGGT-3'; human *KLF4*: forward 5'-GTTCCCATCTCAAGGCACAC-3', reverse 5'-CCCCGTGTGTTTACGGTAGT-3', and human β–*ACTIN*: forward 5'-AGAGCTACGAGCTGCCTGAC-3', reverse 5'-AGCACTGTGTTGGCGTACAG-3'. The relative levels of gene expression were determined through normalization to the levels of an endogenous control: the expression of *B2m*, *Gapdh* or β–*ACTIN* was quantified by comparison with the control.

Statistical analysis

The data are shown as the mean ± standard deviation (s.d.). F-tests followed by two-tailed Student's *t*-tests were used to analyze the results of two groups. For comparison of multiple groups, Tukey's test

was performed using MEPHAS (http://www.gen-info.osaka-u.ac.jp/testdocs/tomocom/dunnett-e.html). The p-values < 0.05 denoted statistically significant differences.

Results

bFGF broke the quiescence of SMCs but not ECs

Contact inhibition, in which growth arrest is obtained by cell–cell contact, and serum deprivation lead to quiescence in non-cancerous cells [8]. To investigate the factors which trigger the disruption of the stable sheet-like appearance of a vascular cell monolayer (referred to as "quiescence breakage" in this report), we performed serum-free confluent culture of the mouse SMC line MOVAS cells and the mouse EC line UV2 cells. Confluent cell layers were treated with ACTIVIN A (20 ng/ml), BMP4 (100 ng/ml), CXCL12 (20 ng/ml), EPO (2 U/ml), FGFa (10 ng/ml), bFGF (20 ng/ml), IGF-II (100 ng/ml), IL-3 (20 ng/ml), PDGF-BB(10 ng/ml), SCF (100 ng/ml), SHH (20 ng/ml), TGFβ1 (10 ng/ml), VEGF (20 ng/ml) or WNT-3A (20 ng/ml) in serum-free medium for three days. Microscope images showed tight sheet-like monolayers of flat polygonal-shaped MOVAS cells and epithelial-like–shaped UV2 cells in the untreated controls (Fig. 1A). Despite known effects of the tested factors on vascular cells (Table 1, 2), most factors did not affect the quiescent MOVAS and UV2 monolayers (Fig. 1). Only bFGF disrupted the quiescent appearance in the MOVAS monolayer, leading to changes in the morphology (i.e., small spindle shapes) and the new formation of a cell-free area (Fig. 1). However, the bFGF had no effect on the quiescent UV2 monolayer.

Immunofluorescent staining of β-catenin, a component of adherens junctions, was employed to examine the details of cell morphology. Treatment with bFGF caused a morphological change in MOVAS cells (Fig. 2A), namely a decrease in cell size compared with Control and TGFβ1 (Fig. 2B). The cell-free areas on the culture surfaces were newly spread in MOVAS monolayers treated with bFGF compared with Control and TGFβ1 (Fig. 2C). Moreover, the cell number was increased by bFGF compared with Control and TGFβ1 (Fig. 2D).

In UV2, there were no significant differences observed between the Control, bFGF, and TGFβ1 groups in cell size (Fig. 2A, B), cell-free area (Fig. 2C), and cell number (Fig. 2D). These results suggest that bFGF broke the established cell quiescence in a cell type–specific manner.

bFGF-induced smooth muscle change, which was accompanied by reduction of TAGLN

The actin-bundling protein TAGLN is abundantly expressed in differentiated SMCs [15], and recognized as one of the myogenic differentiation markers. Differentiated SMCs have a quiescent contractile phenotype with low proliferation rate and high levels of myogenic markers (for a review, see [16]). When SMCs undergo dedifferentiation, they show a change in cell shape, a high proliferation rate and low expression of myogenic markers, resulting in an active synthetic phenotype. TAGLN expression is suppressed during the process of dedifferentiation (for a review, see [16]). In the control MOVAS cells, TAGLN was co-localized with filamentous actin in the polygonal cytoplasm (Fig.3A). bFGF caused strong accumulation of actin at the margins (Fig. 3A) and decreased the co-localization of TAGLN compared with Control and TGFβ1 (Fig. 3B). TGFβ1 induced prominent filamentous actin (Fig. 3A), and the co-localization of TAGLN with actin was similar to that noted in the controls (Fig. 3B). SMC dedifferentiation is characterized by a transition to a proliferative phenotype with a reduction of SMC markers, including TAGLN (for a review, see [16]). Therefore, these findings imply that bFGF-induced breakage of quiescence results in the proliferative dedifferentiation of SMCs.

TAGLN expression also has been described in non-SMCs including mesenchymal cells, kidney cell lines or ECs [17] [18] [19][13]. TAGLN was also present in UV2 cells and co-localized with filamentous actin in the cytoplasm in the controls (Fig. 3C). Treatment with bFGF or TGFβ1 did not have a significant effect on the co-localization of TAGLN compared with the controls (Fig. 3D), suggesting that the effect of bFGF on TAGLN distribution may be specific to SMCs.

bFGF decreased the expression of *Tagln* and *Srf* genes in SMCs but not ECs

FGF binds to and activates the receptor tyrosine kinase FGFR (for a review, see [20]). The expression of *Fgfr1* (coding for FGFR1, a high affinity receptor for bFGF) was assessed to rule out the possibility that the non-response of the UV2 monolayer to bFGF may be due to the lack of FGFR1. *Fgfr1* was fully and highly expressed in MOVAS and UV2 cells compared with B16 cells (Fig. 4A). These results indicated that bFGF may be specifically involved in the breakage of quiescence of SMCs, regardless of the presence of the receptor. Moreover, consistent with the expression of TAGLN proteins (Fig. 3), the significant transcriptional activity of the *Tagln* promoter was detected in MOVAS and UV2 cells (Fig. 4B). bFGF downregulated the expression of *Tagln* and *Srf* genes in MOVAS cells compared with Control. TGFβ1 upregulated the expression of *Tagln* and *Klf4* genes compared with Control (Fig. 4C). The expression levels of *Tagln*, *Srf*, and *Klf4* genes were not significantly different in UV2 cells treated with Control, bFGF, or TGFβ1 (Fig. 4C). SRF and Klf4 are important transcription factors for SMC differentiation [21] [22]. Therefore, bFGF and TGFβ1 regulate the expression of *Srf* and *Klf4*, respectively. Consequently, they may contribute to the transcription of *Tagln* in quiescent SMCs.

Of note, bFGF and TGFβ1 appear to exert opposite effects on *Tagln* transcription (Fig. 4C). Therefore, we investigated whether the effect of bFGF can be reversed by TGFβ1. Co-treatment with bFGF and TGFβ1 disrupted quiescence in the MOVAS monolayer and caused a similar morphological change to that induced by single treatment with bFGF (Fig. 5). This evidence demonstrated that TGFβ1 failed to prevent the breakage of quiescence induced by bFGF. The features of the UV2 monolayer were not affected by bFGF with or without TGFβ1 (Fig. 5).

bFGF broke the quiescence of human primary SMCs but not of human primary ECs

We extended our study by using human primary SMCs (AoSMCs) and human primary ECs (HUVECs) to confirm the effects of bFGF. Confluent primary cell layers were treated with bFGF (20 ng/ml) or TGFβ1 (10 ng/ml) in low serum medium for three days. In the untreated controls, AoSMCs showed tight sheet-like monolayers of polygonal-shaped cells (Fig. S1). HUVECs showed a dispersed population of endothelial-shaped cells, as some cells could not survive under low serum condition

(Fig. S1). bFGF caused most AoSMCs to shift to a small round shape, but some cells remained polygonal. bFGF did not affect the shape of HUVECs. TGFβ1 had no effect on cell shapes in AoSMCs or HUVECs. The β-catenin staining showed that bFGF reduced cell size and increased the number of cells in AoSMCs compared with Control and TGFβ1 (Fig. S2). HUVECs showed no significant alteration of cell size and cell number during treatment with Control, bFGF, or TGFβ1 (Fig. S2). TAGLN co-localized with actin in AoSMCs and HUVECs in the untreated controls (Fig. S3). The co-localized area in AoSMCs were decreased by bFGF, and increased by TGFβ1. No significant difference in the co-localization ratio was found in HUVECs in the Control, bFGF, or TGFβ1 groups. The expression of *TAGLN* gene in AoSMCs were decreased by bFGF and increased by TGFβ1, which generally correlate with the expression of SRF and KLF4 genes (Fig. S4A). These gene expression levels were not significantly different in HUVECs in the three groups (Fig. S4B).

These results with AoSMCs and HUVECs appear to be consistent with the results for MOVAS and UV2 cells. Furthermore, co-treatment of TGFβ1 also did not reverse the effect of bFGF in AoSMCs (Fig. S5). These findings suggest that bFGF may exert a unique effect on SMC lineages in a quiescent state.

Discussion

In this study, we performed screening of factors in serum-free confluent cultures of an SMC line or an EC line to identify potential factors involved in the breakage of vascular cell quiescence. We found that bFGF triggered the disruption of quiescence in the SMC monolayer, but not in the EC monolayer. Treatment with bFGF induced morphological changes and proliferation, accompanied by reduction of the SMC marker. This suggests that bFGF caused SMC-specific breakage of quiescence, almost simultaneously a proliferative dedifferentiation. Similar effects of bFGF were also observed in human primary SMCs and human primary ECs in low serum confluent cultures. Although it has been reported that numerous factors regulate the proliferation or migration of SMCs in varied cellular contexts

(Table 1), our screening demonstrated that only bFGF altered quiescent appearance in the SMC monolayer. Therefore, breakage of SMC-quiescence may be a unique process specifically triggered by bFGF.

bFGF is a member of the family of heparin-binding proteins, and a mitogen for various cell types including SMCs and ECs [23] (for a review, see [24]). Antisense inhibition of endogenous bFGF suppressed DNA synthesis, and induced apoptosis in rat aortic SMCs [25] [26]. bFGF and TGFβ1 antagonistically regulate myogenic differentiation. The expression of *Tagln* in 10T1/2 cells, rat aortic SMCs, and human airway SMCs was upregulated by TGFβ1; notably, these effects were neutralized by bFGF [27] [28]. Interference with FGF signaling using *Fgfr1* siRNA increased TGFβ signaling activity in human aortic SMCs cultured for a long period of time in low-serum medium [29]. Our results showed the opposite effect of bFGF and TGFβ on *Tagln* transcription. However, interestingly, the bFGF-induced breakage of quiescence was not inhibited by TGFβ1. The cellular responses to TGFβ have been reported to be influenced by cellular contexts such as cell-type, cell density or the presence of other factors [30] [31]. TGFβ1 promoted mitosis induced by bFGF in confluent rat aortic SMCs [31]. These findings suggest that the responses of SMCs rely on cellular contexts, such as cell density [30].

The transcription of myogenic genes, including *Tagln*, is regulated by SRF and KLF4 via binding to CArG boxes and TGFβ1 control element sites [32] [33] (for a review, see [34]). SRF and KLF4 act pleiotropically in the presence of bFGF and TGFβ1 [27] [21] [35] [33] [36]. Our results showed that *Tagln* expression corresponded to significant changes in the *Srf* and *Klf4* genes in SMCs stimulated with bFGF and TGFβ1, suggesting a putative transcriptional regulation of *Tagln*.

VEGF is an essential factor for endothelial activation. We also have previously shown the role of VEGF in vascular-tube formation *in vitro* [37] [38] [39], and vascular development *in vivo* [40] [41] (for reviews, see [42] [43]). bFGF stimulates proliferation and migration of ECs [44] (for a review, see [45]). TGFβ1 attenuated EC proliferation and promoted tube formation [46]. Despite the known

effects of factors (e.g., VEGF, bFGF and TGF1) on ECs (Table 2), our screening did not reveal factors associated with the breakage of quiescence in ECs. Although the FGF receptor was more abundant in ECs than SMCs, bFGF exerted SMC-specific effects. These findings appear to resemble an early histological event of atherosclerosis with proliferation of SMCs, but not ECs. Synergistic effects of CXCL12 and VEGF, or BMP4 and heat shock protein (HSP) 70 have been reported in promotion of proliferation, migration, or tube-formation [47] [48]. Therefore, the breakage of quiescence in the EC monolayer may require other stimuli or multiple factors. Further studies are warranted to investigate the mechanisms involved in this process.

Tagln has widely accepted to be a canonical marker of SMCs. Therefore, ECs expressing *Tagln* are conventionally recognized as undergoing endothelial-to-mesenchymal transition (EndMT). EndMT has been observed in pathological vascular conditions including atherosclerosis (for a review, see [4]). TGFβ has been reported to induce EndMT, which is augmented or attenuated by bFGF in the various contexts. The feature of EndMT *in vitro* is derived under certain stimulation such as a mechanical strain or a prolonged culture, in which ECs express SMC markers and show morphological changes [49] [50]. On the other hand, we recently detected activated transcription of *Tagln* in elongated ECs under angiogenic stimuli [13]. It has been reported that *Tagln* expression is induced following the contact and spreading of mesenchymal cells on an adherent surface [17] [18]; *Tagln* is sensitive to changes in the morphology of non-SMCs. Therefore, the elevated expression of *Tagln* may be related to physiological morphological changes in ECs, in addition to pathological processes such as EndMT. Consistent with this line of thought, the present results showed that ECs with unchanged morphology expressed similar levels of *Tagln* regardless of bFGF and TGFβ1.

SMCs have multiple and independent developmental origins including mesoderm and neural crest (for a review, see [51], and are well known to exhibit phenotypic heterogeneity in various parameters including cell shape, marker expression, proliferative activity and cellular responses to stimuli [52] (for a review, see [53]). Our study showed that MOVAS cells were highly uniform in shape under bFGF treatment, while AoSMCs had some mixture of the different cell shapes. This may be due to the

property of MOVAS cells as a single-clone cell line and the heterogeneity of the primary cell population of AoSMCs. Although the bFGF-induced morphological change in AoSMCs was not as prominent as in MOVAS cells, it was similarly associated with the proliferation and dedifferentiation. On the other hand, ECs are recognized to arise from the mesoderm, and erythro-myeloid progenitors (EMPs) were recently reported as one of the origins (for a review, see [54]). ECs have a strong heterogeneity depending on organs and within the capillaries of each organ (for a review, see [55]), and HUVECs also do [56]. In the current study, HUVECs appear to contain at least two populations which were sensitive and insensitive to a low serum condition, respectively. The surviving cells were not affected by bFGF and TGFβ1, similar to UV2 cells. Our study suggests that the cell lines may represent a part of the heterogeneous properties in primary cell populations, and serum-free confluent culture of the cell lines may be useful to examine cellular responses in the quiescent state.

In this report, we showed that bFGF caused breakage of quiescence in SMCs and led to proliferative dedifferentiation. These bFGF-induced effects may be cell-type specific and may be a unique response independent of that shared with other factors (Table 1, 2). The phenotypic transition of SMCs is a key component of atherosclerosis. Our results may provide a new insight into bFGF as a potent trigger of dysfunction in SMCs.

Data Availability

The data that support the findings of this study are available from the corresponding author [ktamuratsuji@den.hokudai.ac.jp] upon reasonable request.

Acknowledgements

This work was supported by KAKENHI [grant number: 18K0978208] from the Japan Society for the Promotion of Science (JSPS).

Conflict of Interest Statement

The authors declare that they have no competing interests.

Author Contributions

K. Tsuji-Tamura designed and performed research, and analyzed data. M. Tamura helped perform experiments. All authors wrote the paper.

References

1 Conway EM, Collen D & Carmeliet P (2001) Molecular mechanisms of blood vessel growth. *Cardiovasc Res* **49**, 507–521.

2 Neese RA, Misell LM, Turner S, Chu A, Kim J, Cesar D, Hoh R, Antelo F, Strawford A, Mccune JM, Christiansen M & Hellerstein MK (2002) Measurement in vivo of proliferation rates of slow turnover cells by 2 H 2 O labeling of the deoxyribose moiety of DNA. *Proceedings of the National Academy of Sciences of the United States of America* **99**, 15345–15350.

3 Hobson B & Denekamp J (1984) Endothelial proliferation in tumours and normal tissues: Continuous labelling studies. *Br J Cancer* **49**, 405–413.

4 Low EL, Baker AH & Bradshaw AC (2019) TGFβ smooth muscle cells and coronary artery disease: a review. *Cellular Signalling* **53**, 90–101.

5 Theodorou K & Boon RA (2018) Endothelial cell metabolism in atherosclerosis. *Frontiers in Cell and Developmental Biology* **6**.

6 Liekens S, de Clercq E & Neyts J (2001) Angiogenesis: regulators and clinical applications. *Biochemical Pharmacology* **61**, 253–270.

7 Muto A, Fitzgerald TN, Pimiento JM, Maloney SP, Teso D, Paszkowiak JJ, Westvik TS, Kudo FA, Nishibe T & Dardik A (2007) Smooth muscle cell signal transduction: Implications of vascular biology for vascular surgeons. *Journal of Vascular Surgery* **45**, 15a–24a.

8 Gos M, Miloszewska J, Swoboda P, Trembacz H, Skierski J & Janik P (2005) Cellular quiescence induced by contact inhibition or serum withdrawal in C3H10T1/2 cells. *Cell Proliferation* **38**, 107–116.

9 Saltis J, Thomasb AC, Agrotis A, Campbellb JH, Campbellb GR, Bobik A & Alfred-Baker " " (1995) Expression of growth factor receptors on arterial smooth muscle cells. Dependency on cell phenotype and serum factors. *Atherosclerosis* **118**, 77–87.

10 Wen J-K, Han M, Zheng B & Yang S-L (2002) Comparison of gene expression patterns and migration capability at quiescent and proliferating vascular smooth muscle cells stimulated by cytokines. *Life Sciences* **70**, 799–807.

11 Stavri GT, Zachary IC, Baskerville PA, Martin JF & Erusalimsky JD (1995) Basic Fibroblast Growth-Factor up-Regulates the Expression of Vascular Endothelial Growth-Factor in Vascular Smooth-Muscle Cells - Synergistic Interaction with Hypoxia. *Circulation* **92**, 11–14.

12 Fontijn RD, Volger OL, Fledderus JO, Reijerkerk A, de Vries HE & Horrevoets AJG (2008) SOX-18 controls endothelial-specific claudin-5 gene expression and barrier function. *Am J Physiol Heart Circ Phys-iol* **294**, 891–900.

13 Tsuji-Tamura K, Morino-Koga S, Suzuki S & Ogawa M (2021) The canonical smooth muscle cell marker TAGLN is present in endothelial cells and is involved in angiogenesis. *Journal of Cell Science* **134**.

14 Akyurek LM, Yang ZY, Aoki K, San H, Nabel GJ, Parmacek MS & Nabel EG (2000) SM22alpha promoter targets gene expression to vascular smooth muscle cells in vitro and in vivo. *Mol Med* **6**, 983–991.

15 Lees-Miller JP, Heeley DH & Smillie LB (1987) *An abundant and novel protein of 22 kDa (SM22) is widely distributed in smooth muscles Purification from bovine aorta*.

16 Doevendans PA & van Eys G (2002) Smooth muscle cells on the move: the battle for actin. *Cardiovascular Research* **54**, 499–502.

17 Shapland C, Lowings P & Lawson D (1988) Identification of new actin-associated polypeptides that are modified by viral transformation and changes in cell shape. *Journal of Cell Biology* **107**, 153–161.

18 Shapland C, Hsuan JJ, Totty NE & Lawson D (1993) Purification and Properties of Transgelin: A Transformation and Shape Change Sensitive Actin-gelling Protein. *J Cell Biol* **121**, 1065–1073.

19 Chen J, Kitchen CM, Streb JW & Miano JM (2002) Myocardin: A Component of a Molecular Switch for Smooth Muscle Differentiation. *Journal of Molecular and Cellular Cardiology* **34**, 1345–1356.

20 Eswarakumar VP, Lax I & Schlessinger J (2005) Cellular signaling by fibroblast growth factor receptors. *Cytokine and Growth Factor Reviews* **16**, 139–149.

21 Nishida W, Nakamura M, Mori S, Takahashi M, Ohkawa Y, Tadokoro S, Yoshida K, Hiwada K, Hayashi K & Sobue K (2002) A triad of serum response factor and the GATA and NK families governs the transcription of smooth and cardiac muscle genes. *Journal of Biological Chemistry* **277**, 7308–7317.

22 Wassmann S, Wassmann K, Jung A, Velten M, Knuefermann P, Petoumenos V, Becher U, Werner C, Mueller C & Nickenig G (2007) Induction of p53 by GKLF is essential for inhibition of proliferation of vascular smooth muscle cells. *Journal of Molecular and Cellular Cardiology* **43**, 301–307.

23 Davis MG, Zhou M, Ali S, Coffin JD, Doetschman T & Dorn GW (1997) Intracrine and autocrine effects of basic fibroblast growth factor in vascular smooth muscle cells. *Journal of Molecular and Cellular Cardiology* **29**, 1061–1072.

24 Chung J & Shum-Tim D (2012) Neovascularization in Tissue Engineering. *Cells* **1**, 1246–1260.

25 Fox JC & Shanley JR (1996) Antisense inhibition of basic fibroblast growth factor induces apoptosis in vascular smooth muscle cells. *Journal of Biological Chemistry* **271**, 12578–12584.

26 Itoh H, Mukoyama M, Pratt RE, Gibbons GH & Dzau VJ (1993) Multiple autocrine growth factors modulate vascular smooth muscle cell growth response to angiotensin II. *Journal of Clinical Investigation* **91**, 2268–2274.

27 Kawai-Kowase K, Sato H, Oyama Y, Kanai H, Sato M, Doi H & Kurabayashi M (2004) Basic fibroblast growth factor antagonizes transforming growth factor-β1-induced smooth muscle gene expression through extracellular signal-regulated kinase 1/2 signaling pathway activation. *Arteriosclerosis, Thrombosis, and Vascular Biology* **24**, 1384–1390.

28 Schuliga M, Javeed A, Harris T, Xia Y, Qin C, Wang Z, Zhang X, Lee PVS, Camoretti-Mercado B & Stewart AG (2013) Transforming growth factor-β-Induced differentiation of airway smooth muscle cells is inhibited by fibroblast growth factor-2. *American Journal of Respiratory Cell and Molecular Biology* **48**, 346–353.

29 Chen PY, Qin LF, Li GX, Tellides G & Simons M (2016) Fibroblast growth factor (FGF) signaling regulates transforming growth factor beta (TGF beta)-dependent smooth muscle cell phenotype modulation. *Scientific Reports* **6**.

30 Majack RA (1987) Beta-Type Transforming Growth Factor Specifies Organizational Behavior in Vascular Smooth Muscle Cell Cultures. *The Journal of Cell Biology* **106**, 465–471.

31 Majack RA, Majesky MW & Goodman L v (1990) Role of PDGF-A Expression in the Control of Vascular Smooth Muscle Cell Growth by Transforming Growth Factor. *TheJournalof Cell Biology* **111**, 239–247.

485 32 Kim S, Ip HS, Lu MM, Clendenin C & Parmacek MS (1997) A Serum Response Factor-Dependent
486 Transcriptional Regulatory Program Identifies Distinct Smooth Muscle Cell Sublineages.
487 *MOLECULAR AND CELLULAR BIOLOGY* **17**, 2266–2278.
488 33 Adam PJ, Regan CP, Hautmann MB & Owens GK (2000) Positive- and negative-acting Kruppel-
489 like transcription factors bind a transforming growth factor β control element required for
490 expression of the smooth muscle cell differentiation marker SM22α in vivo. *Journal of*
491 *Biological Chemistry* **275**, 37798–37806.
492 34 Kumar MS & Owens GK (2003) Combinatorial control of smooth muscle-specific gene expression.
493 *Arteriosclerosis, Thrombosis, and Vascular Biology* **23**, 737–747.
494 35 Qiu P, Feng XH & Li L (2003) Interaction of Smad3 and SRF-associated complex mediates TGF-
495 β1 signals to regulate SM22 transcription during myofibroblast differentiation. *Journal of*
496 *Molecular and Cellular Cardiology* **35**, 1407–1420.
497 36 Li HX, Han M, Bernier M, Zheng B, Sun SG, Su M, Zhang R, Fu JR & Wen JK (2010) Krüppel-
498 like factor 4 promotes differentiation by transforming growth factor-β receptor-mediated Smad
499 and p38 MAPK signaling in vascular smooth muscle cells. *Journal of Biological Chemistry* **285**,
500 17846–17856.
501 37 Park S-H, Sakamoto H, Tsuji-Tamura K, Furuyama T & Ogawa M (2009) Foxo1 is essential for in
502 vitro vascular formation from embryonic stem cells. *Biochemical and Biophysical Research*
503 *Communications* **390**.

504 38 Tsuji-Tamura K & Ogawa M (2018) Dual inhibition of mTORC1 and mTORC2 perturbs
505 cytoskeletal organization and impairs endothelial cell elongation. *Biochemical and Biophysical*
506 *Research Communications* **497**, 326–331.
507 39 Tsuji-Tamura K & Ogawa M (2016) Inhibition of the PI3K-Akt and mTORC1 signaling pathways
508 promotes the elongation of vascular endothelial cells. *Journal of Cell Science* **129**, 1165–1178.
509 40 Tsuji-Tamura K, Sato M, Fujita M & Tamura M (2020) Glycine exerts dose-dependent biphasic
510 effects on vascular development of zebrafish embryos. *Biochemical and Biophysical Research*
511 *Communications* **527**, 539–544.
512 41 Tsuji-Tamura K, Sato M, Fujita M & Tamura M (2020) The role of PI3K/Akt/mTOR signaling in
513 dose-dependent biphasic effects of glycine on vascular development. *Biochemical and*
514 *Biophysical Research Communications* **529**, 596–602.
515 42 Tsuji-Tamura K, Sakamoto H & Ogawa M (2011) ES Cell Differentiation as a Model to Study Cell
516 Biological Regulation of Vascular Development. In *Embryonic Stem Cells: The Hormonal*
517 *Regulation of Pluripotency and Embryogenesis (ed. C. S. Atwood)* pp. 581–606.
518 43 Tsuji-Tamura K & Ogawa M (2018) Morphology regulation in vascular endothelial cells.
519 *Inflammation and Regeneration* **38**.
520 44 Jih YJ, Lien WH, Tsai WC, Yang GW, Li C & Wu LW (2001) Distinct regulation of genes by bFGF
521 and VEGF-A in endothelial cells. *Angiogenesis* **4**, 313–321.

45 Lamalice L, le Boeuf F & Huot J (2007) Endothelial cell migration during angiogenesis. *Circulation Research* **100**, 782–794.

46 Madri JA, Pratt BM & Tucker AM (1988) Phenotypic Modulation of Endothelial Cells by Transforming Growth Factor-13 Depends upon the Composition and Organization of the Extracellular Matrix. *J Cell Biol* **106**, 1375–1384.

47 Kryczek I, Lange A, Mottram P, Alvarez X, Cheng P, Hogan M, Moons L, Wei S, Zou L, Machelon V, Emilie D, Terrassa M, Lackner A, Curiel TJ, Carmeliet P & Zou W (2005) CXCL12 and Vascular Endothelial Growth Factor Synergistically Induce Neoangiogenesis in Human Ovarian Cancers. *Cancer Res* **65**, 465–472.

48 Yao Y, Watson AD, Ji S & Boström KI (2009) Heat shock protein 70 enhances vascular bone morphogenetic protein-4 signaling by binding Matrix Gla protein. *Circulation Research* **105**, 575–584.

49 Cevallos M, Riha GM, Wang X, Yang H, Yan S, Li M, Chai H, Yao Q & Chen C (2006) Cyclic strain induces expression of specific smooth muscle cell markers in human endothelial cells. *Differentiation* **74**, 552–561.

50 Frid MG, Kale VA & Stenmark KR (2002) Mature vascular endothelium can give rise to smooth muscle cells via endothelial-mesenchymal transdifferentiation: In vitro analysis. *Circulation Research* **90**, 1189–1196.

51 Majesky MW, Dong XR, Regan JN & Hoglund VJ (2011) Vascular smooth muscle progenitor cells: Building and repairing blood vessels. *Circulation Research* **108**, 365–377.

52 Hao H, Ropraz P, Verin V, Camenzind E, Geinoz A, Pepper MS, Gabbiani G & Bochaton-Piallat ML (2002) Heterogeneity of smooth muscle cell populations cultured from pig coronary artery. *Arteriosclerosis, Thrombosis, and Vascular Biology* **22**, 1093–1099.

53 Gittenberger-De Groot AC, Deruiter MC, Bergwerff M & Poelmann RE (1999) *Smooth Muscle Cell Origin and Its Relation to Heterogeneity in Development and Disease*.

54 Iruela-Arispe M (2018) A dual origin for blood vessels. *Nature* **562**, 195–197.

55 Hennigs JK, Matuszcak C, Trepel M & Körbelin J (2021) Vascular endothelial cells: Heterogeneity and targeting approaches. *Cells* **10**.

56 Turgeon PJ, Chan GC, Chen L, Jamal AN, Yan MS, Ho JJD, Yuan L, Ibeh N, Ku KH, Cybulsky MI, Aird WC & Marsden PA (2020) Epigenetic Heterogeneity and Mitotic Heritability Prime Endothelial Cell Gene Induction. *The Journal of Immunology* **204**, 1173–1187.

57 Kojima I, Mogami H, Norio KN, Horoshi YH & Shibata H (1993) Modulation of Growth of Vascular Smooth Muscle Cells by Activin A. *Experimental Cell Research* **206**, 152–156.

58 Frank DB, Abtahi A, Yamaguchi DJ, Manning S, Shyr Y, Pozzi A, Baldwin HS, Johnson JE & de Caestecker MP (2005) Bone morphogenetic protein 4 promotes pulmonary vascular remodeling in hypoxic pulmonary hypertension. *Circulation Research* **97**, 496–504.

59 Pan CH, Chen CW, Sheu MJ & Wu CH (2012) Salvianolic acid B inhibits SDF-1α-stimulated cell proliferation and migration of vascular smooth muscle cells by suppressing CXCR4 receptor. *Vascular Pharmacology* **56**, 98–105.

60 Park SL, Won SY, Song JH, Kambe T, Nagao M, Kim WJ & Moon SK (2015) EPO gene expression promotes proliferation, migration and invasion via the p38MAPK/AP-1/MMP-9 pathway by p21WAF1 expression in vascular smooth muscle cells. *Cellular Signalling* **27**, 470–478.

61 Ghiselli G, Chen J, Kaou M, Hallak H & Rubin R (2003) Ethanol inhibits fibroblast growth factor-induced proliferation of aortic smooth muscle cells. *Arteriosclerosis, Thrombosis, and Vascular Biology* **23**, 1808–1813.

62 Yang N, Dong B, Song Y, Li Y, Kou L, Yang J & Qin Q (2020) Downregulation of miR-637 promotes vascular smooth muscle cell proliferation and migration via regulation of insulin-like growth factor-2. *Cellular and Molecular Biology Letters* **25**.

63 Brizzi MF, Formato L, Dentelli P, Rosso A, Pavan M, Garbarino G, Pegoraro M, Camussi G & Pegoraro L (2001) Interleukin-3 Stimulates Migration and Proliferation of Vascular Smooth Muscle Cells A Potential Role in Atherogenesis. *Circulation* **103**, 549–545.

64 Li L, Blumenthal DK, Terry CM, He Y, Carlson ML & Cheung AK (2011) PDGF-induced proliferation in human arterial and venous smooth muscle cells: Molecular basis for differential effects of PDGF isoforms. *Journal of Cellular Biochemistry* **112**, 289–298.

577 65 Wang CH, Verma S, Hsieh IC, Hung A, Cheng TT, Wang SY, Liu YC, Stanford WL, Weisel RD, Li
578 RK & Cherng WJ (2007) Stem cell factor attenuates vascular smooth muscle apoptosis and
579 increases intimal hyperplasia after vascular injury. *Arteriosclerosis, Thrombosis, and Vascular*
580 *Biology* **27**, 540–547.
581 66 Li F, Duman-Scheel M, Yang D, Du W, Zhang J, Zhao C, Qin L & Xin S (2010) Sonic hedgehog
582 signaling induces vascular smooth muscle cell proliferation via induction of the G1 cyclin-
583 retinoblastoma axis. *Arteriosclerosis, Thrombosis, and Vascular Biology* **30**, 1787–1794.
584 67 Grosskreutz CL, Anand-Apte B, Dupláa C, Quinn TP, Terman BI, Zetter B & D'amore PA (1999)
585 Vascular Endothelial Growth Factor-Induced Migration of Vascular Smooth Muscle Cells in
586 Vitro. *Microvasc Res* **58**, 128–136.
587 68 Carthy JM, Luo Z & McManus BM (2012) WNT3A induces a contractile and secretory phenotype
588 in cultured vascular smooth muscle cells that is associated with increased gap junction
589 communication. *Laboratory Investigation* **92**, 246–255.
590 69 Kaneda H, Arao T, Matsumoto K, de Velasco MA, Tamura D, Aomatsu K, Kudo K, Sakai K, Nagai
591 T, Fujita Y, Tanaka K, Yanagihara K, Yamada Y, Okamoto I, Nakagawa K & Nishio K (2011)
592 Activin A inhibits vascular endothelial cell growth and suppresses tumour angiogenesis in gastric
593 cancer. *British Journal of Cancer* **105**, 1210–1217.
594 70 Zhang M, Qiu L, Zhang Y, Xu D, Zheng JC & Jiang L (2017) CXCL12 enhances angiogenesis
595 through CXCR7 activation in human umbilical vein endothelial cells. *Scientific Reports* **7**.

71 Carlini RG, Reyes AA & Romsmin M (1995) Recombinant human erythropoietin stimulates angiogenesis in vitro. *Kidney International* **47**, 740–745.

72 Anagnostou A, Lee ES, Kessimian N, Levinsont R & Steiner M (1990) Erythropoietin has a mitogenic and positive chemotactic effect on endothelial cells (hematopoietic growth factors). *Proc Natd Acad Sci USA* **87**, 5978–5982.

73 Giraux J-L, Matoua S, Brosa A, Tapon-Bretaudierea J, Letourneur D & Fischer1 A-M (1998) Modulation of human endothelial cell proliferation and migration by fucoidan and heparin. *European Journal of Cell Biology* **77**, 352–359.

74 Brizzi MF, Garbarino G, Rossi PR, Pagliardi GL, Arduino C, Avanzi GC & Pegoraro L (1993) Interleukin 3 stimulates proliferation and triggers endothelial-leukocyte adhesion molecule 1 gene activation of human endothelial cells. *J Clin Invest* **91**, 2887–2892.

75 Dallinga MG, Habani YI, Kayser RP, van Noorden CJF, Klaassen I & Schlingemann RO (2020) IGF-binding proteins 3 and 4 are regulators of sprouting angiogenesis. *Molecular Biology Reports* **47**, 2561–2572.

76 Battegay EJ, Rupp J, Iruela-Arispe L, Sage EH & Pech M (1994) PDGF-BB Modulates Endothelial Proliferation and Angiogenesis In Vitro via PDGF B-Receptors. *The Journal of Cell Biology* **125**, 917–928.

77 Phillips GD & Stone AM (1994) *PDGF-BB induced chemotaxis is impaired in aged capillary endothelial cells*.

78 Broudy VC, Kovach NL, Bennett LG, Lin N, Jacobsen FW & Kidd PG (1994) Human Umbilical Vein Endothelial Cells Display High-Affinity c-kit Receptors and Produce a Soluble Form of the c-kit Receptor. *Blood* **83**, 2145–2152.

79 Rivron NC, Raiss CC, Liu J, Nandakumar A, Sticht C, Gretz N, Truckenmüller R, Rouwkema J & van Blitterswijk CA (2012) Sonic Hedgehog-activated engineered blood vessels enhance bone tissue formation. *Proc Natl Acad Sci USA* **109**, 4413–4418.

80 Cross MJ & Claesson-Welsh L (2001) FGF and VEGF function in angiogenesis: signalling pathways, biological responses and therapeutic inhibition. *TRENDS in Pharmacological Sciences* **22**, 201–207.

81 Samarzija I, Sini P, Schlange T, MacDonald G & Hynes NE (2009) Wnt3a regulates proliferation and migration of HUVEC via canonical and non-canonical Wnt signaling pathways. *Biochemical and Biophysical Research Communications* **386**, 449–454.

Figure Legends

Figure 1. bFGF broke the quiescence of SMCs, but not ECs

At confluence, the mouse vascular smooth muscle cell line (MOVAS) and the mouse vascular endothelial cell line (UV2) were treated with the indicated factor for three days in serum-free medium. (A) Images of MOVAS and UV2 cells. The white arrow points to MOVAS cells with changed shape after treatment with bFGF. The white asterisk denotes a cell-free area. The final concentration of each factor is indicated in the bracket of each panel. Scale bars show 100 μm. Similar results were obtained in three independent experiments. (B) Proportion of MOVAS cells with different shapes (flat

polygonal shape, and others including small spindle shape), and of UV2 cells (epithelial-like shape and others) found in each group (n = 300 from three independent experiments). bFGF, basic fibroblast growth factor; BMP4, bone morphogenetic protein 4; CXCL12, chemokine (C-X-C motif) ligand 12; EPO, erythropoietin; FGFa, FGF acidic; IGF-II, insulin-like growth factor-II; IL-3, interleukin-3; PDGF-BB, platelet-derived growth factor-bb; SCF, stem cell factor; SHH, sonic hedgehog; TGFβ1, transforming growth factor beta 1; VEGF, vascular endothelial growth factor; WNT-3A, wingless-type MMTV integration site family, member-3A.

Figure 2. bFGF reduced cell size and increased proliferation in SMCs

Confluent MOVAS and UV2 cells were treated with bFGF (20 ng/ml) or TGFβ1 (10 ng/ml) for three days in serum-free medium. (A) Fluorescent images after staining with β-catenin (gray) and DAPI (blue). Scale bars show 50 μm. Similar results were observed in three independent experiments. (B) Cell size. Data are presented as the mean ± s.d. (n = 100 from three independent experiments). * $p <$ 0.05 by Tukey's test. (C) Cell-free area per image. Data are presented as the mean ± s.d. (n = 9 from three independent experiments). * $p < 0.05$ by Tukey's test. (D) Cell number per image. Data are presented as the mean ± s.d. (n = 9 from three independent experiments). * $p < 0.05$ by Tukey's test.

Figure 3. bFGF-induced SMC changes accompanied by reduced co-localization of TAGLN and actin

Confluent MOVAS or UV2 cells were treated with bFGF (20 ng/ml) or TGFβ1 (10 ng/ml) for three days in serum-free medium. (A and C) Fluorescent images after staining with β-catenin (gray), actin (green), and TAGLN (red). Scale bars show 20 μm. Similar results were observed in three independent experiments. (B and D) Co-localization area of TAGLN and actin per image. Data are presented as the mean ± s.d. (n = 9 from three independent experiments). * $p < 0.05$ by Tukey's test.

Figure 4. bFGF decreased the expression of *Tagln* and *Srf* in SMCs, but not ECs

(A) The expression of *Fgfr1* in B16, MOVAS, and UV2 cells was quantified using real-time PCR. *B2m* was used for normalization. Data are presented as the mean ± s.d. (n = 5 from three independent

experiments). * $p < 0.05$ by Tukey's test. (B) Luciferase reporter assay of the *Tagln* promoter in MOVAS and UV2 cells. The reporter activity was normalized to that of the co-transfected Renilla luciferase plasmid. Data are presented as the mean ± s.d. (n = 5 per group). ** $p < 0.01$ versus pGL4.15 vector control by the F-test, followed by Student's *t*-test. Similar results were obtained in three independent experiments. (C) Confluent MOVAS and UV2 cells were treated with bFGF (20 ng/ml) or TGFβ1 (10 ng/ml) for three days in serum-free medium. The expression of *Tagln*, *Srf*, and *Klf4* was quantified using real-time PCR. *B2m* or *Gapdh* was used for the normalization of *Tagln* and *Klf4*, or *Srf*, expression. Data are presented as the mean ± s.d. (n = 5 from three independent experiments). * $p < 0.05$ by Tukey's test.

Figure 5. TGFβ1 failed to prevent bFGF-induced breakage of quiescence in SMCs

At confluence, cells were treated with the indicated factor for three days in serum-free medium. (A) Images of MOVAS and UV2 cells. White arrows point to MOVAS cells with changed shapes. White asterisks denote cell-free areas. The final concentration of each factor is indicated in the bracket of each panel. Scale bars show 100 μm. Similar results were obtained in three independent experiments. (B) Proportion of MOVAS cells with different shapes (flat polygonal shape, and others including small spindle shape), and of UV2 cells (epithelial-like shape and others) found in each group, (n = 300 from three independent experiments).

Figure 1

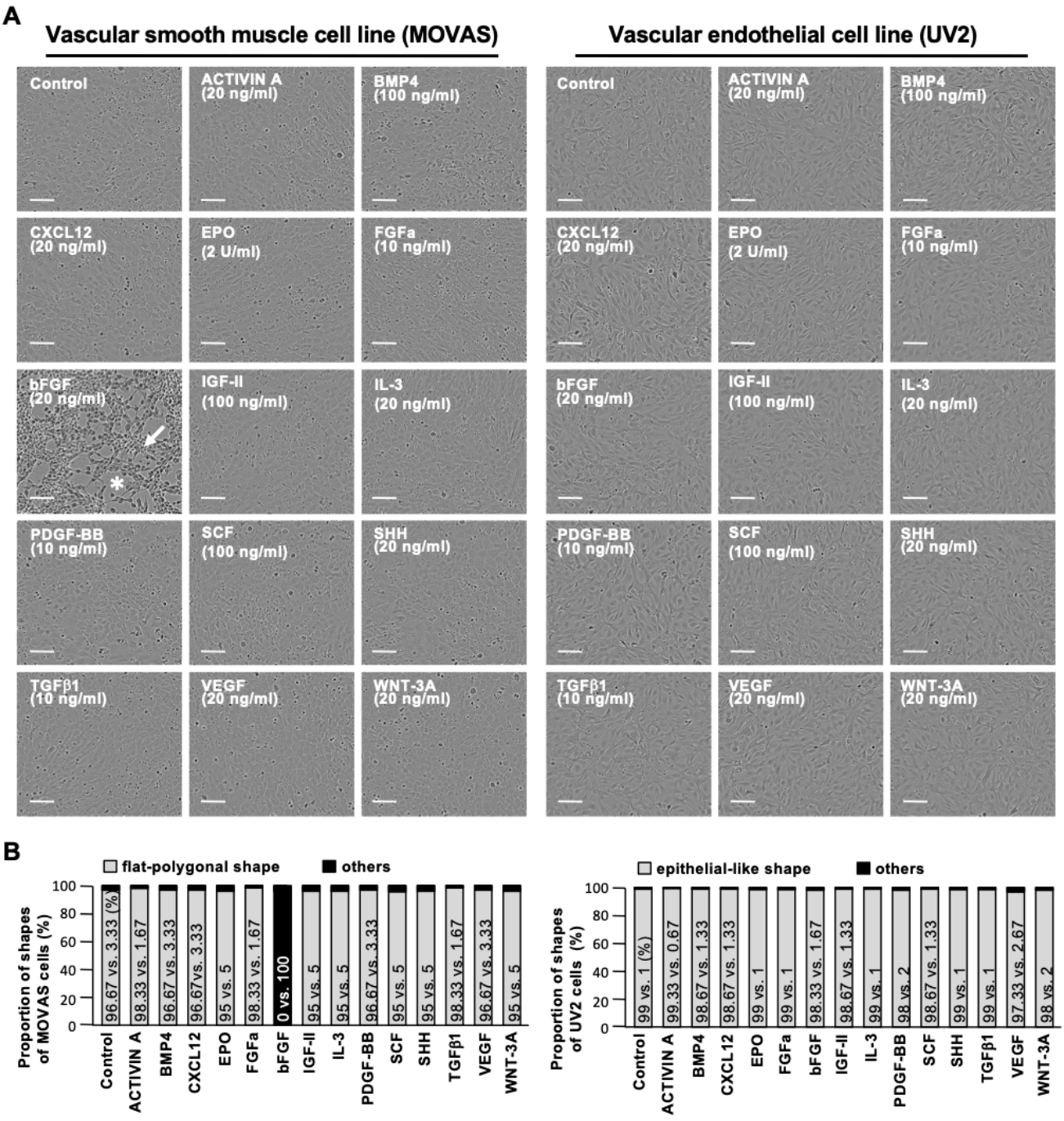
A
Vascular smooth muscle cell line (MOVAS)
Vascular endothelial cell line (UV2)
Control
ACTIVIN A (20 ng/ml)
BMP4 (100 ng/ml)
CXCL12 (20 ng/ml)
EPO (2 U/ml)
FGFa (10 ng/ml)
bFGF (20 ng/ml)
IGF-II (100 ng/ml)
IL-3 (20 ng/ml)
PDGF-BB (10 ng/ml)
SCF (100 ng/ml)
SHH (20 ng/ml)
TGFβ1 (10 ng/ml)
VEGF (20 ng/ml)
WNT-3A (20 ng/ml)
B
flat-polygonal shape
others
Proportion of shapes of MOVAS cells (%)
96.67 vs. 3.33 (%)
98.33 vs. 1.67
96.67 vs. 3.33
96.67vs. 3.33
95 vs. 5
98.33 vs. 1.67
0 vs. 100
95 vs. 5
95 vs. 5
96.67 vs. 3.33
95 vs. 5
95 vs. 5
98.33 vs. 1.67
96.67 vs. 3.33
95 vs. 5
epithelial-like shape
others
Proportion of shapes of UV2 cells (%)
99 vs. 1 (%)
99.33 vs. 0.67
98.67 vs. 1.33
98.67 vs. 1.33
99 vs. 1
99 vs. 1
98.33 vs. 1.67
98.67 vs. 1.33
99 vs. 1
98 vs. 2
98.67 vs. 1.33
99 vs. 1
99 vs. 1
97.33 vs. 2.67
98 vs. 2

Figure 2

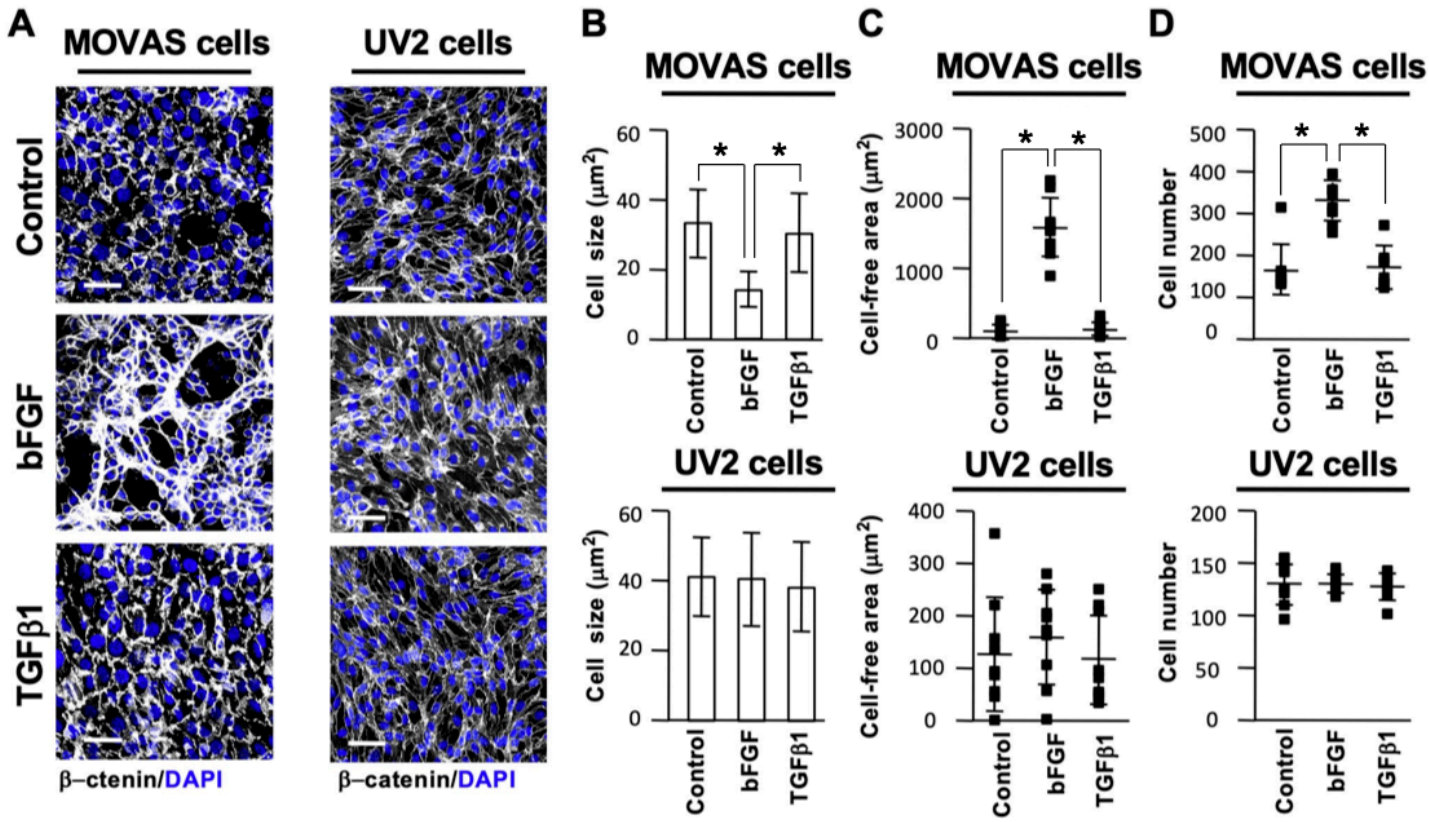
A
MOVAS cells
UV2 cells
Control
bFGF
TGFβ1
β–ctenin/DAPI
β–catenin/DAPI
B
MOVAS cells
Cell size (μm²)
UV2 cells
C
MOVAS cells
Cell-free area (μm²)
UV2 cells
D
MOVAS cells
Cell number
UV2 cells
Control
bFGF
TGFβ1

Figure 3

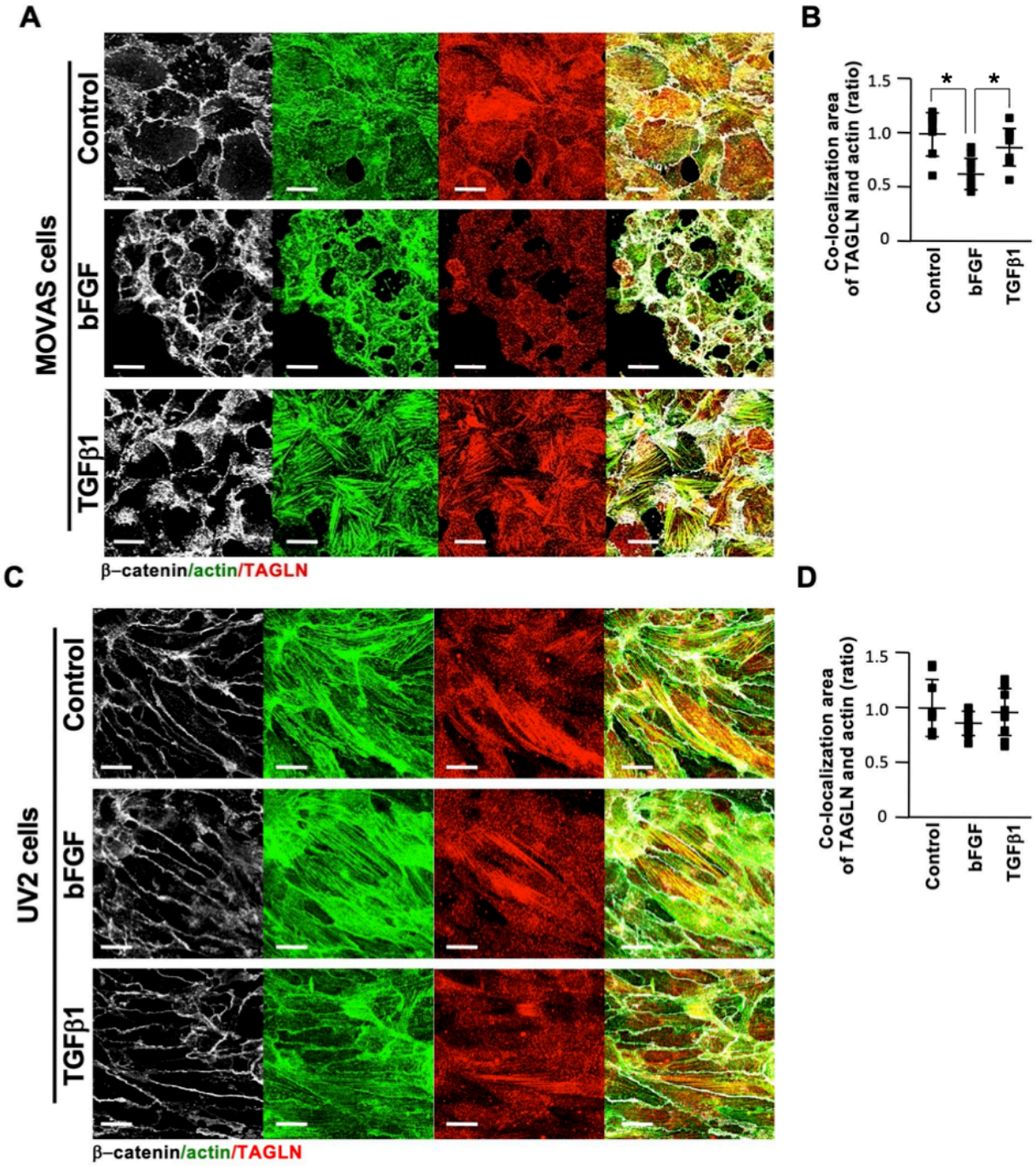
A
MOVAS cells
Control
bFGF
TGFβ1
β–catenin/actin/TAGLN
B
Co-localization area of TAGLN and actin (ratio)
1.5
1.0
0.5
0
*
*
Control
bFGF
TGFβ1
C
UV2 cells
Control
bFGF
TGFβ1
β–catenin/actin/TAGLN
D
Co-localization area of TAGLN and actin (ratio)
1.5
1.0
0.5
0
Control
bFGF
TGFβ1

Figure 4

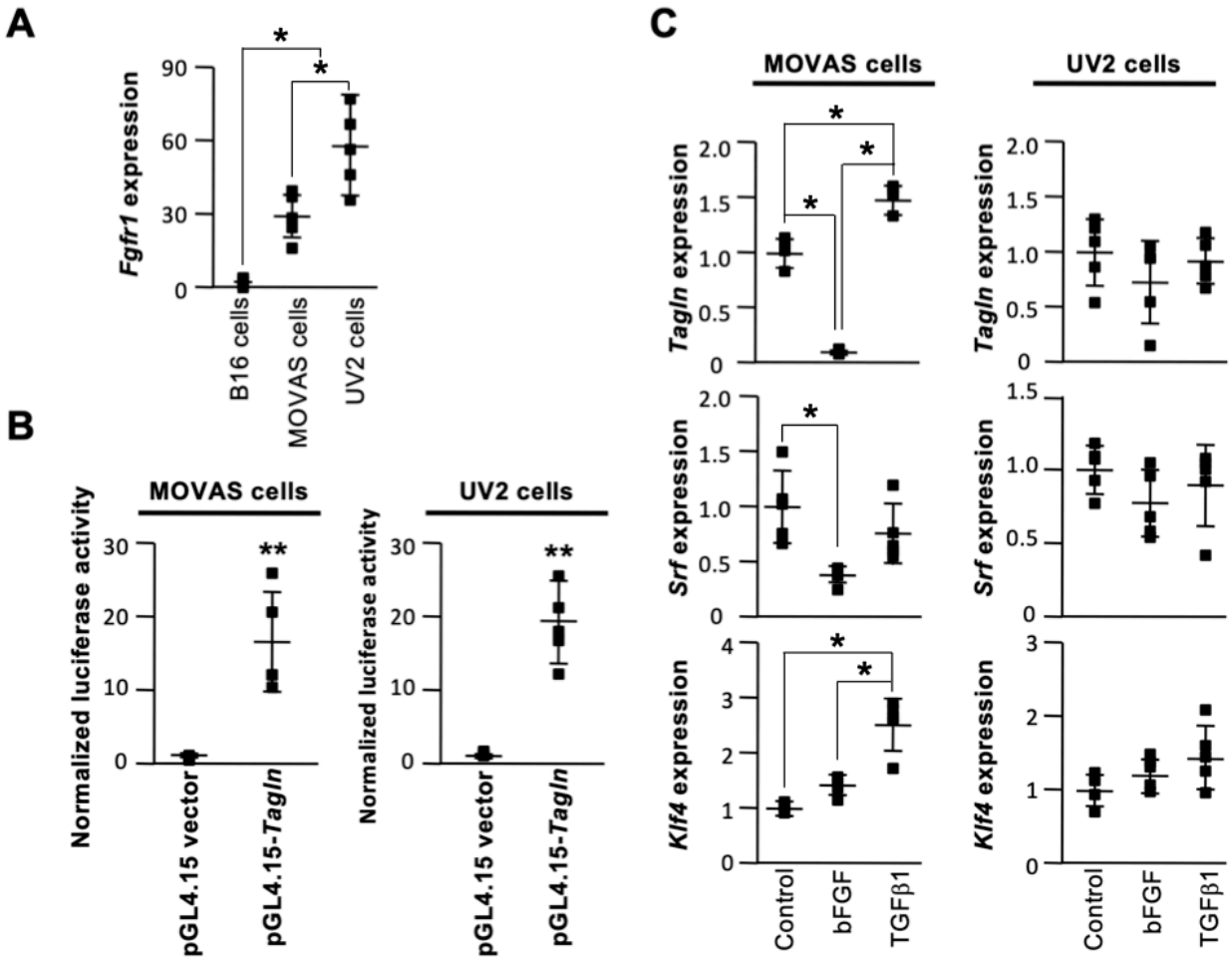
A
Fgfr1 expression
90
60
30
0
B16 cells
MOVAS cells
UV2 cells
B
MOVAS cells
UV2 cells
Normalized luciferase activity
30
20
10
0
pGL4.15 vector
pGL4.15-Tagln
C
MOVAS cells
UV2 cells
Tagln expression
Srf expression
Klf4 expression
Control
bFGF
TGFβ1

Figure 5

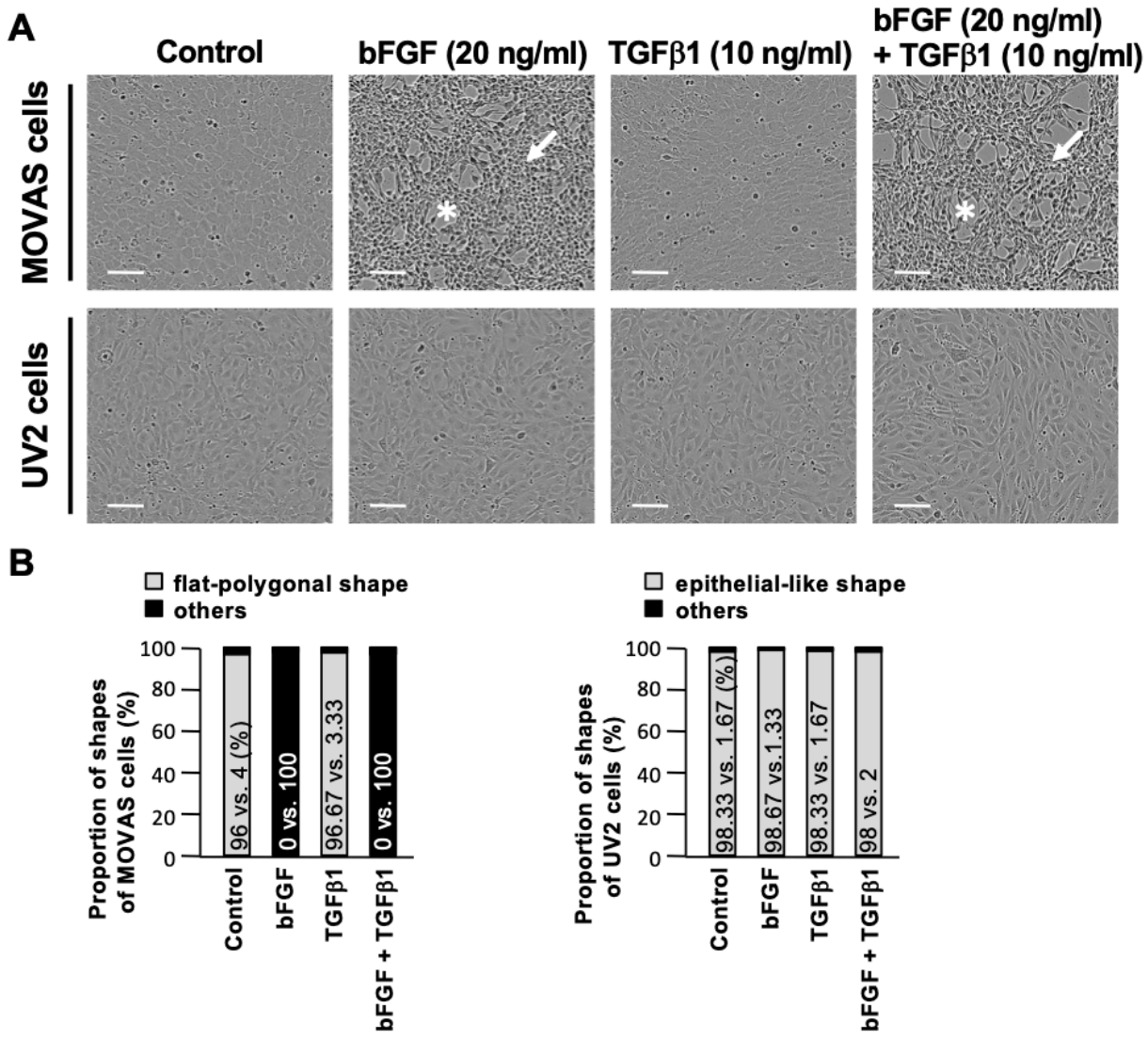
A
Control
bFGF (20 ng/ml)
TGFβ1 (10 ng/ml)
bFGF (20 ng/ml) + TGFβ1 (10 ng/ml)
MOVAS cells
UV2 cells
B
flat-polygonal shape
others
Proportion of shapes of MOVAS cells (%)
100
80
60
40
20
0
96 vs. 4 (%)
0 vs. 100
96.67 vs. 3.33
0 vs. 100
Control
bFGF
TGFβ1
bFGF + TGFβ1
epithelial-like shape
others
Proportion of shapes of UV2 cells (%)
98.33 vs. 1.67 (%)
98.67 vs.1.33
98.33 vs. 1.67
98 vs. 2
Control
bFGF
TGFβ1
bFGF + TGFβ1

Supplementary Figures

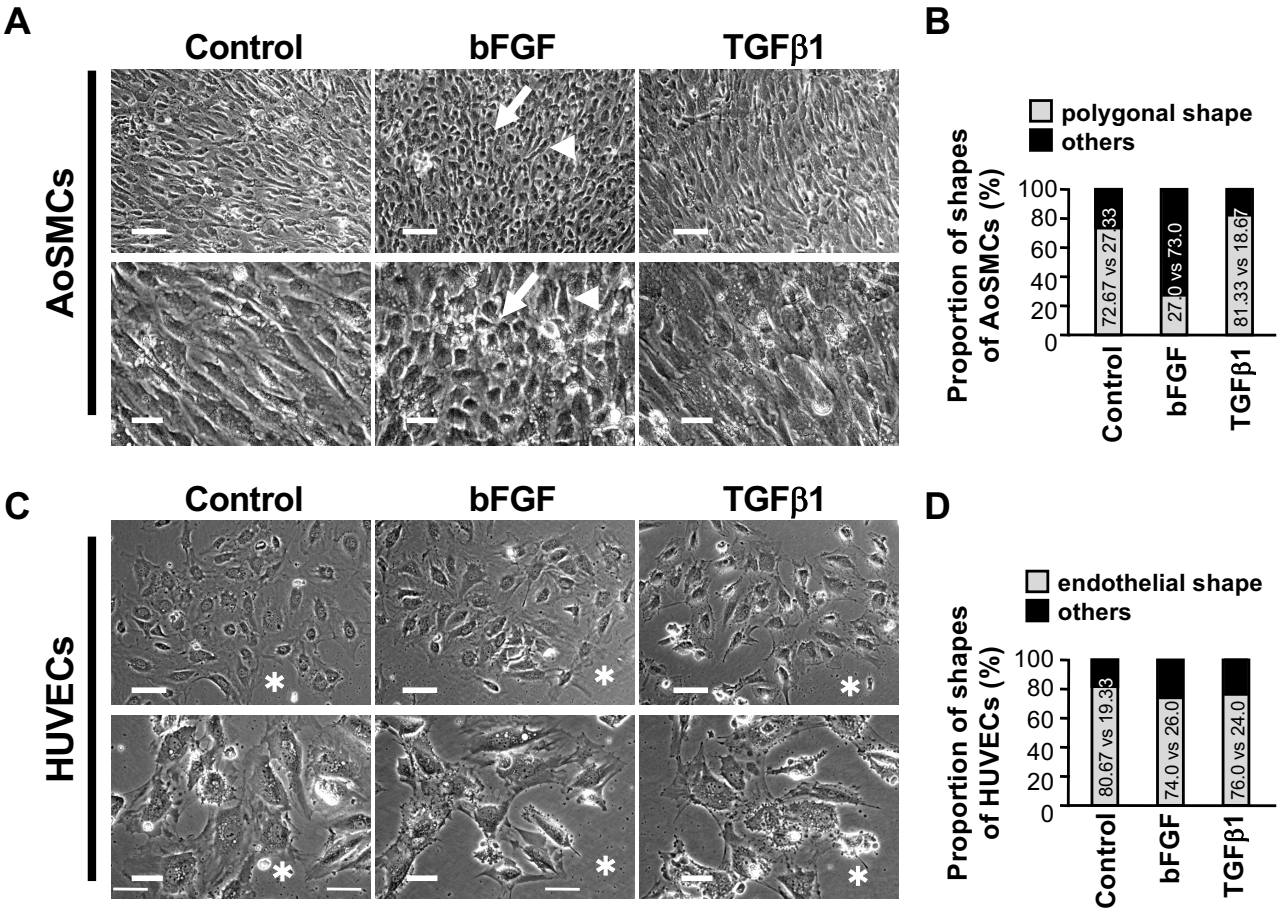

Fig. S1. bFGF broke the quiescence of human primary SMCs, but not human primary ECs
At confluence, human aortic smooth muscle cells (AoSMCs) and human umbilical vein endothelial cells (HUVECs) were treated with the bFGF (20 ng/ml) or TGFβ1 (10 ng/ml) for three days in 0.1% FBS medium (low serum medium). (A and C) Images of AoSMCs and HUVECs. White arrows point to AoSMCs with changed shape after treatment with bFGF, and white arrowheads point to polygonal shaped cells. The white asterisks denote cell-free spaces probably formed by the death of some HUVECs due to low serum stimulation. Scale bars show 90 μm (upper panels) and 40 μm (lower panels). Similar results were obtained in three independent experiments. (B and D) The proportion of AoSMCs with different shapes (polygonal shape, and others including small round shape), and of HUVECs (endothelial shape and others) found in each group (n = 300 from three independent experiments).

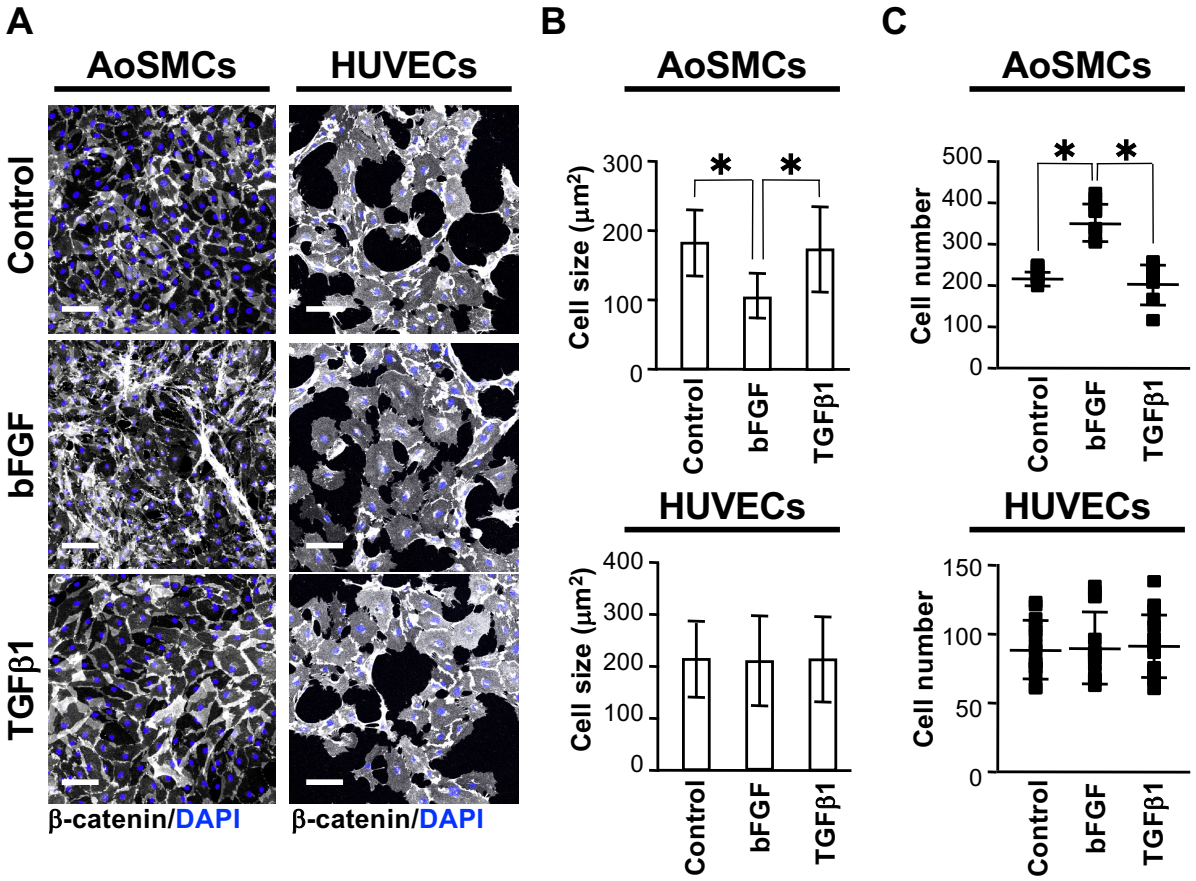

Fig. S2. bFGF reduced cell size and increased proliferation in primary SMCs
Confluent AoSMCs and HUVECs were treated with bFGF (20 ng/ml) or TGFβ1 (10 ng/ml) for three days in low serum medium. (A) Fluorescent images after staining with β-catenin (gray) and DAPI (blue). Scale bars show 100 μm. Similar results were observed in three independent experiments. (B) Cell size. Data are presented as the mean ± s.d. (n = 300 from three independent experiments). * $p < 0.05$ by Tukey's test. (C) Cell number per image. Data are presented as the mean ± s.d. [n = 9 (AoSMCs) or 15 (HUVECs) from three independent experiments]. * $p < 0.05$ by Tukey's test.

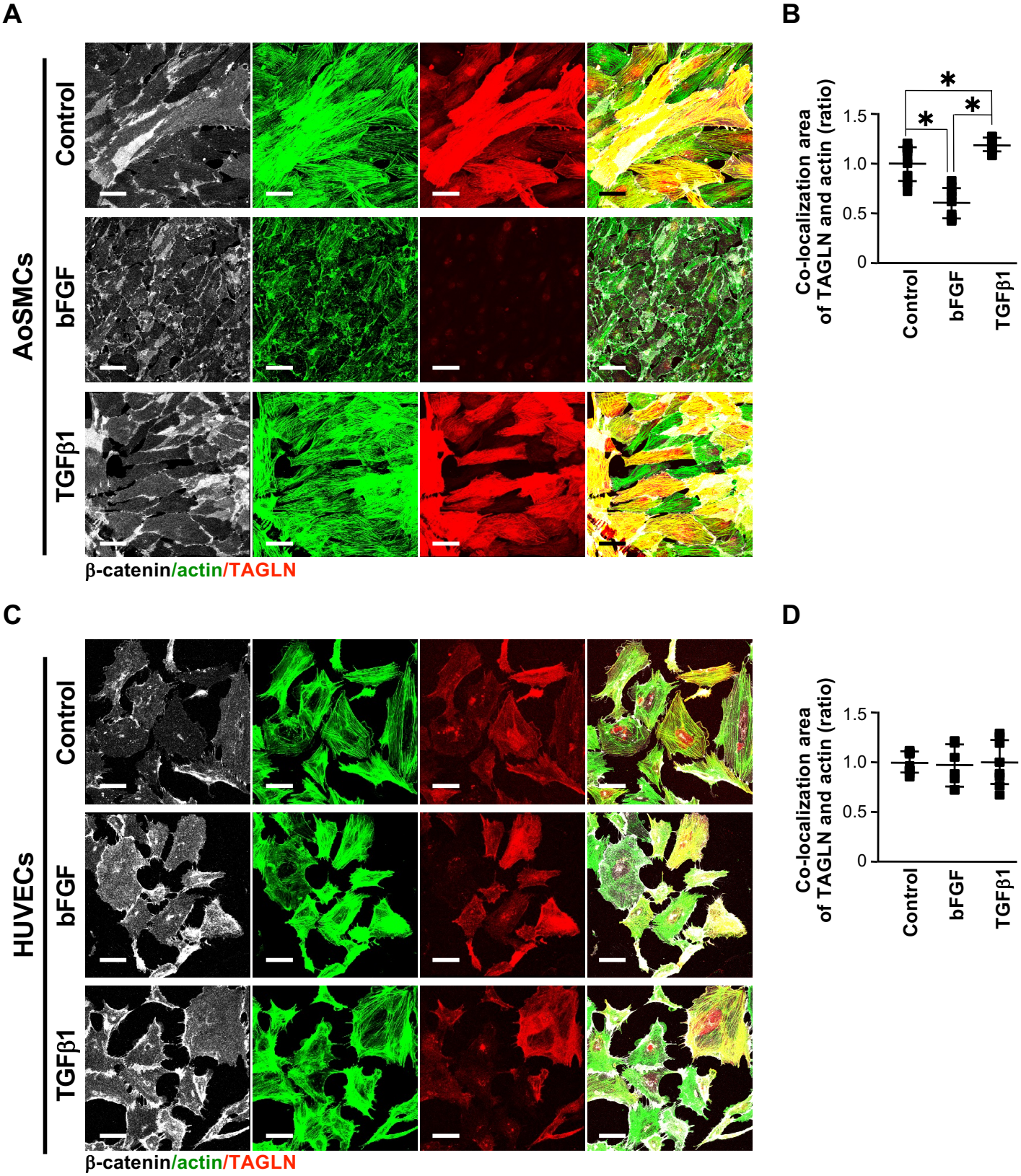

Fig. S3. bFGF-induced primary SMCs changes accompanied by reduced co-localization of TAGLN and actin

Confluent AoSMCs and HUVECs were treated with bFGF (20 ng/ml) or TGFβ1 (10 ng/ml) for three days in low serum medium. (A and C) Fluorescent images after staining with β-catenin (gray), actin (green), and TAGLN (red). Scale bars show 50 μm. Similar results were observed in three independent experiments. (B and D) Co-localization area of TAGLN and actin per image. Data are presented as the mean ± s.d. (n = 9 from three independent experiments). * $p < 0.05$ by Tukey's test.

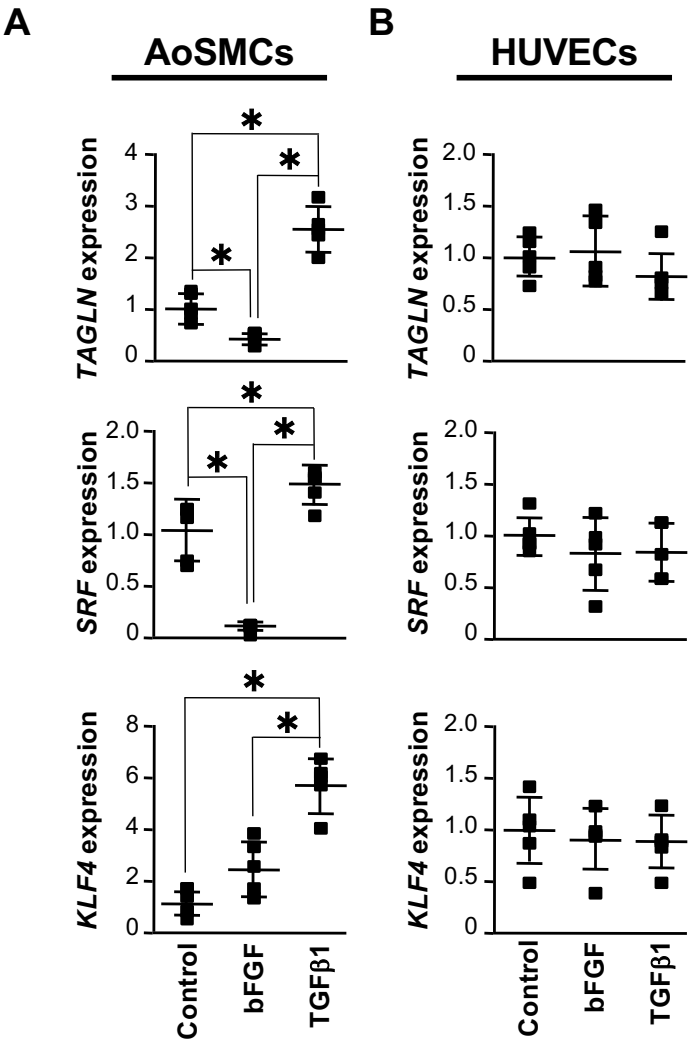

Fig. S4. bFGF decreased the expression of *TAGLN* and *SRF* in primary SMCs.
Confluent AoSMCs and HUVECs were treated with bFGF (20 ng/ml) or TGFβ1 (10 ng/ml) for three days in low serum medium. The expression of *TAGLN*, *SRF*, and *KLF4* was quantified using real-time PCR. *beta-ACTIN* was used for the normalization of gene expression. Data are presented as the mean ± s.d. (n = 5 from three independent experiments). * $p < 0.05$ by Tukey's test.

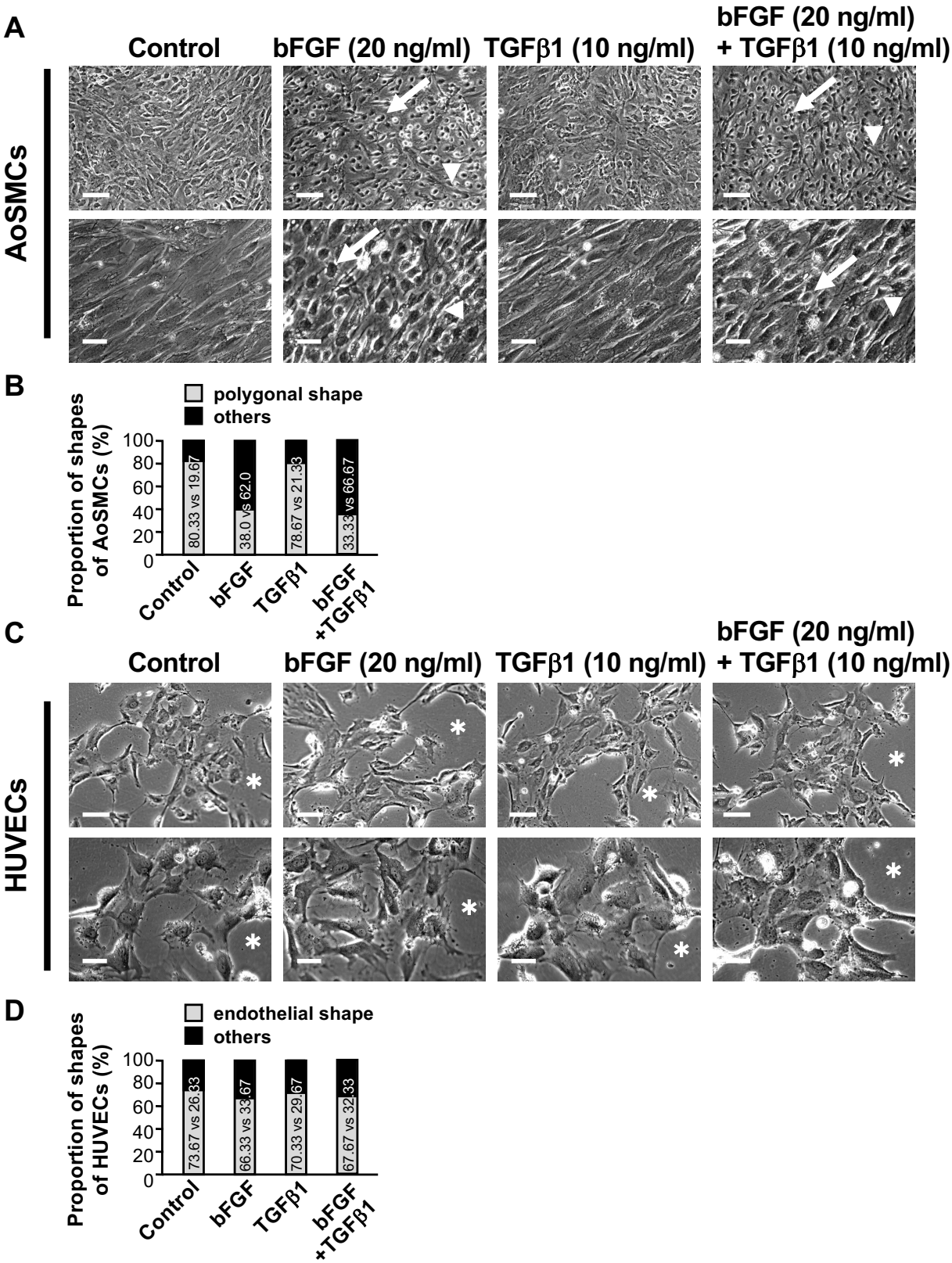

Fig. S5. TGFβ1 failed to prevent bFGF-induced breakage of quiescence in primary SMCs

At confluence, cells were treated with the indicated factor for three days in low serum medium. (A and C) Images of AoSMCs and HUVECs. White arrows point to AoSMCs with changed shape after treatment with bFGF without or with TGFβ1, and white arrowheads point to polygonal shaped cells. The white asterisks denote cell-free spaces probably formed by the death of some HUVECs due to low serum stimulation. The final concentration of each factor is indicated in the bracket of each panel. Scale bars show 90 μm (upper panels) and 40 μm (lower panels). Similar results were obtained in three independent experiments. (B and D) The proportion of AoSMCs with different shapes (polygonal shape, and others including small round shape), and of HUVECs (endothelial shape and others) found in each group (n = 300 from three independent experiments).

Graphical Abstract

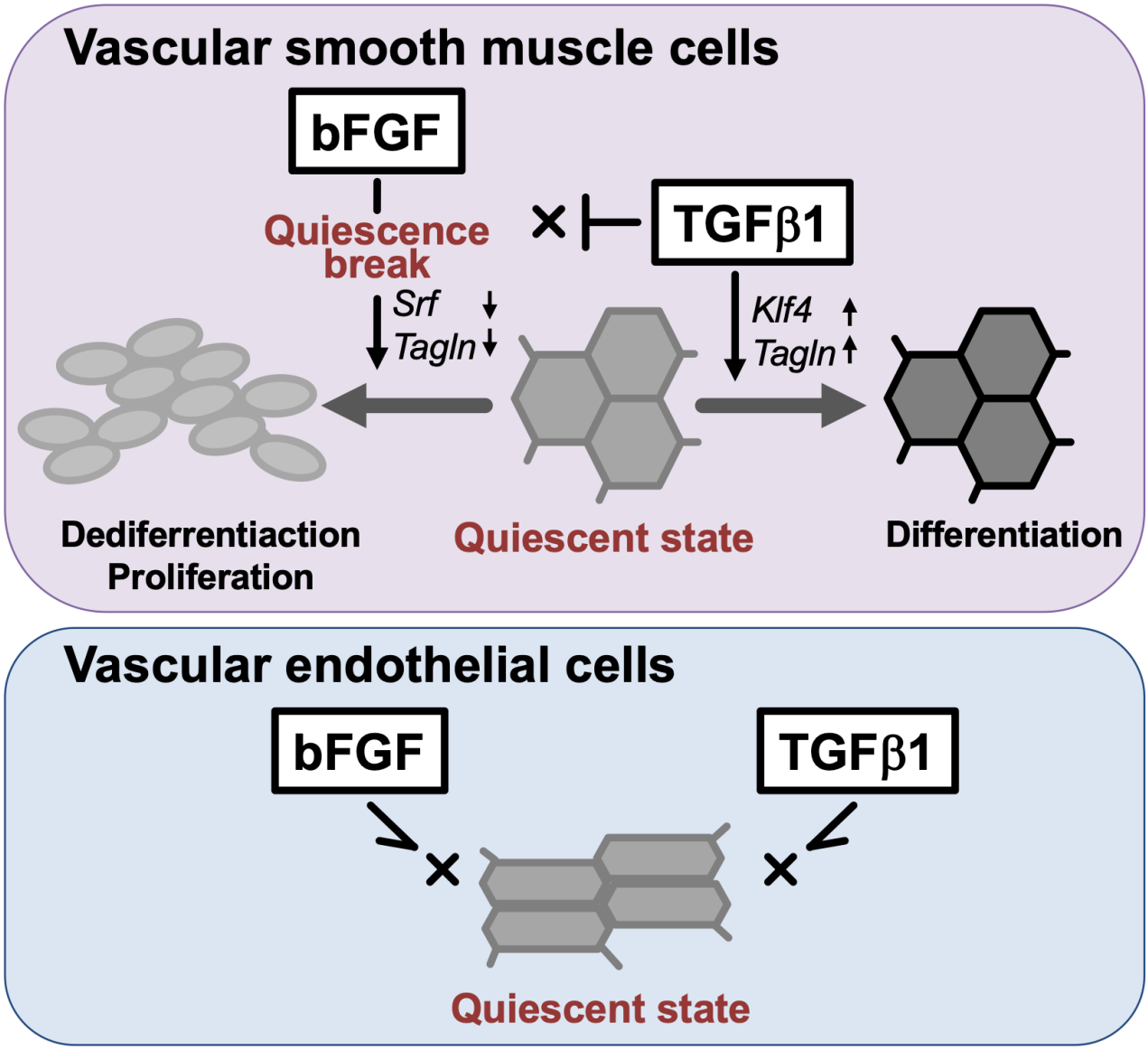

bFGF induced breakage of quiescence in vascular smooth muscle cells, and led to dedifferentiation and proliferation accompanied by reduced expression of a transcription factor *Srf* and a myogenic marker *Tagln*. TGFβ1 upregulated a transcription factor *Klf4* and *Tagln* expression and induced differentiation; however, it failed to inhibit bFGF-induced quiescence breakage. bFGF and TGFβ1 didn't affect the quiescent vascular endothelial cells.